Journal of Materials Chemistry C

ROYAL SOCIETY OF CHEMISTRY

PAPER

View Article Online
View Journal | View Issue

Check for updates

Cite this: J. Mater. Chem. C, 2023, 11, 1429

A nonalternant azulene-embedded carbon nanohoop featuring anti-Kasha emission and tunable properties upon pH stimuli-responsiveness†

Xiaonan Li,[a] Luyang Jia,[a] Wenguang Wang,[a] Ying Wang,[a] Di Sun[b] and Hua Jiang*[a]

Received 11th October 2022,
Accepted 15th December 2022

DOI: 10.1039/d2tc04321a

rsc.li/materials-c

The insertion of a nonalternant π-system into the skeletons of [*n*]cycloparaphenylenes ([*n*]CPPs) can significantly alter their optoelectronic properties. We herein present a nonalternant azulene-embedded carbon nanohoop **1,3-Az[9]CPP**. The investigations revealed that **1,3-Az[9]CPP** demonstrates unique properties including anti-Kasha emission, reversible pH stimuli-responsiveness and tunable band gaps upon protonation and deprotonation. Importantly, **1,3-Az[9]CPP** exhibits a highly selective binding for C_{60} over C_{70} (K_{C60}/K_{C70} = 30) in acidic media. Moreover, the molecular structures of **1,3-Az[9]CPP** and its fullerene complex **C_{60}@1,3-Az[9]CPP** were confirmed by single-crystal X-ray diffraction. Notably, **1,3-Az[9]CPP** is the first pH-responsive nonalternant all-carbon nanohoop, which may hold significant promising applications in tunable optoelectronic materials.

Published on 16 December 2022. Downloaded on 8/16/2024 8:58:14 AM.

Introduction

[*n*]Cycloparaphenylenes ([*n*]CPPs), consisting of a cyclic arrangement of para-linked phenylenes, are the shortest conjugated fragment of armchair carbon nanotubes (CNTs).[1] Since the initial synthesis by Jasti *et al.* in 2008,[2] numerous CPP derivatives have been developed with various functionalities and thus boosted tremendous advances in the fields of host–guest chemistry and materials science,[3] owing to their in-plane radially oriented π-orbitals and size-dependent optoelectronic properties. So far, a majority of CPP derivatives have been synthesized by embedding alternant aromatic units such as naphthalene,[4] anthracene,[5] pyrene,[6] fluorene,[7,8] pyridine,[9] anthraquinone,[10] and graphenoids[11] into the skeletons of CPPs, thus leading to fascinating applications in organic light emitting diodes (OLEDs),[8] molecular machines,[9] and so on.[12,13] In contrast, incorporating nonalternant π-systems into nanohoops can not only reduce the aromaticity of nanohoops, but also lower their band gap, which significantly alters their electronic properties.[14,16] However, there are limited examples of nonalternant nanohoops from rubicene,[14] fluoranthene,[15] and dibenzo[*a*,*e*]pentenyl[16] and a methylene-bridged non-alternant aromatic belt.[17] Therefore, the developments of nonalternant aromatic carbon nanohoops would be complementary to the abovementioned alternant aromatic counterparts and thus hold great significance for their applications in materials science.

Azulene, a nonalternant isomer of naphthalene, consists of an electron-deficient seven-membered ring and an electron-rich five-membered ring, featuring a large dipole moment of 1.08D and a non-mirror symmetric frontier molecular orbital, which eventually lead to anti-Kasha's rule emission from S_2 to S_0.[18] It is noteworthy that the odd positions of azulene are more electron-rich than the even ones, so protonation can readily occur at the C-1 position to form a stable 6π-azulenylium ion under acidic conditions (Fig. 1a).[19] These unique properties endow azulene with great promise for developing advanced materials in organic semiconductors,[20] photoswitches,[21] nonlinear optical materials,[22] chemical sensing, bioimaging,[23] and nonplanar polycyclic aromatic hydrocarbons.[24] However, investigations associated with nonalternant aromatic all-carbon nanohoops with pH reversible stimuli-responsiveness remained largely unexplored to date because of the lack of suitable stimuli-responsive all-carbon building blocks. Most pH active materials normally require heteroatoms such as nitrogen, oxygen, and sulfur as proton acceptors. Therefore, the synthesis of pH-responsive nonalternant all-carbon nanohoops is still challenging.

The reversible changes in color and physicochemical properties upon protonation/deprotonation make azulene an excellent

[a] College of Chemistry, Beijing Normal University, Beijing 100875, P. R. China
[b] School of Chemistry and Chemical Engineering, Shandong University, Jinan 250100, P. R. China

† Electronic supplementary information (ESI) available. CCDC 2177150 and 2177151. For ESI and crystallographic data in CIF or other electronic format see DOI: https://doi.org/10.1039/d2tc04321a

Published on 16 December 2022. Downloaded on 8/16/2024 8:58:14 AM.

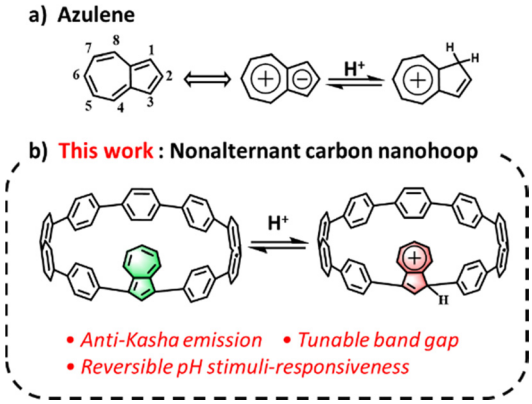

Fig. 1 (a) Azulene and (b) nonalternant azulene-embedded carbon nanohoops used in this work.

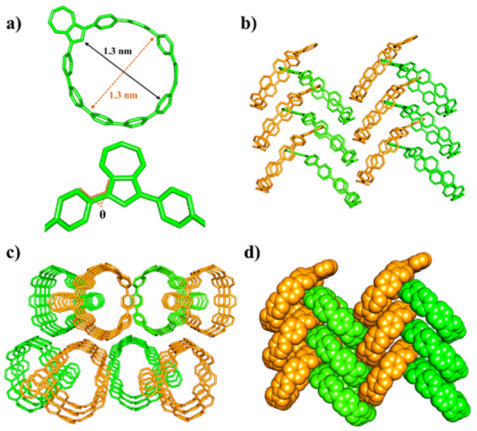

Fig. 2 (a) X-ray crystal structures, (b) herringbone packing model, (c) long range channel alignment and (d) densely stacked **1,3-Az[9]CPP**.

building block for developing pH stimulus-responsive all-carbon nanohoops. We anticipated that incorporating an azulene unit into the CPP backbone would allow us to obtain a nonalternant aromatic all-carbon nanohoop with appealing properties, such as anti-Kasha's rule fluorescence and a tunable band gap upon protonation/deprotonation. Herein, we report the synthesis and structure of novel nonalternant aromatic azulene-embedded [*n*]CPP (**1,3-Az[9]CPP**) (Fig. 1b) and its properties in the absence and presence of acid. Remarkably, the nonalternant aromatic **1,3-Az[9]CPP** displays not only reversible stimuli-responsiveness but also high selectivity for binding C_{60} over C_{70} in acidic media.

Results and discussion

The synthetic procedure for **1,3-Az[9]CPP** is shown in Scheme 1. Our synthetic strategy was to couple two cyclohexadiene fragments **1** and **2** by Suzuki–Miyaura cross-coupling to access dichloride intermediate **3**, followed by Miyaura borylation to give cyclization precursor **4**. In the presence of $Pd(PPh_3)_4$ and K_2CO_3, 1,3-dibromoazulene and C-shaped fragment **4** were subjected to Suzuki–Miyaura cross-coupling in a diluted reaction solution (3.5 mM) to provide the macrocyclic precursor **6**. The final reductive aromatization of the macrocyclic precursor **6** was carried out in anhydrous tetrahydrofuran with freshly prepared H_2SnCl_4 at room temperature, and the target macrocycle **1,3-Az[9]CPP** was obtained in 24% yield over two steps. The structure of **1,3-Az[9]CPP** was confirmed by ^{1}H NMR, ^{13}C NMR, ^{1}H-^{1}H COSY, ^{1}H-^{13}C HSQC, ^{1}H-^{13}C HMBC, MALDI-TOF MS and single-crystal X-ray analysis (Fig. 2, Fig. S1–S7 and S9 and Table S1, ESI†).

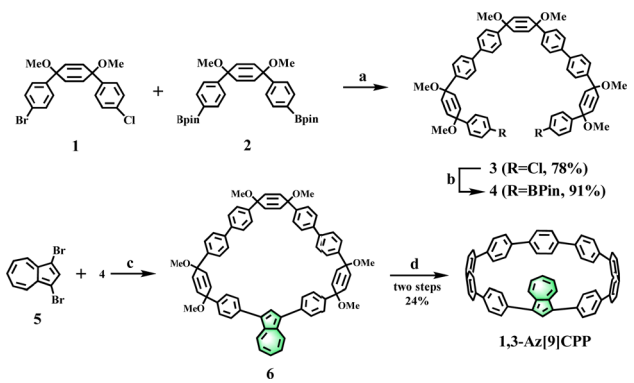

Scheme 1 Synthetic route of **1,3-Az[9]CPP**. Reaction conditions: (a) $Pd(PPh_3)_4$, K_2CO_3, THF/H_2O, 100 °C, 18 h, 78%; (b) B_2pin_2, x-phos, $Pd_2(dba)_3$, KOAc, 1,4-dioxane, 115 °C, overnight, 91%; (c) $Pd(PPh_3)_4$, K_2CO_3, Aliquat 336, toluene/H_2O, 115 °C, 24 h; (d) $SnCl_2$, HCl, THF, r.t., 24 h, 24% in two steps.

The structure of **1,3-Az[9]CPP** was confirmed by single-crystal X-ray analysis (Fig. 2). Suitable crystals were obtained by slow diffusion of acetonitrile into 1,1,2,2-tetrachloroethane solution at room temperature. Crystallographic analysis reveals that the carbon nanohoop exhibits a nearly circular cavity with an estimated diameter of about 1.30 nm (Fig. 2a), which is similar to that of [10]CPP (1.4 nm) and thus enables **1,3-Az[9]CPP** to be a suitable host for fullerenes as [10]CPP.[25] As shown in Fig. 2a, the five-membered ring of azulene points towards the interior of CPP due to the strain caused by the **1,3-Az[9]CPP** nanohoop, thus leading to the formation of dihedral angles of about 45.0° between the azulene unit and the adjacent benzene molecules. **1,3-Az[9]CPP** adopts a herringbone packing in the solid phase when viewed from the side (Fig. 2b and d) and thus forms channels when viewed from the top (Fig. 2c). Furthermore, the unit cell of **1,3-Az[9]CPP** belongs to the $P2_1$ space group.

The ^{1}H NMR spectrum of **1,3-Az[9]CPP** features a set of signals for the azulene protons with δ = 8.70, 7.68, 7.28, and 7.22 ppm for H4/H8, H6, H2, and H5/H7, respectively, and signals for the CPP segment protons with δ = 7.68–7.55 ppm in CD_2Cl_2 (Fig. 3 and Fig. S4, ESI†). Titrations of 0.1–1.5 equiv. $HBArF{\cdot}(Et_2O)_2$ ($BArF^-$: $B[3,5\text{-}(CF_3)_2C_6H_3]_4^-$, *very hygroscopic and sensitive to oxygen*) into the solution of **1,3-Az[9]CPP** caused significant changes in the chemical shifts (Fig. 3 and Fig. S11, ESI†). No further changes were observed for the titrations of $HBArF{\cdot}(Et_2O)_2$ beyond 1.0 equiv. The remarkable downfield shifts of protons assigned to the azulene unit were observed, with the largest downfield shift being assigned to the H5 or H7, up to 1.78 ppm. These significant downfield shifts indicate

 This journal is © The Royal Society of Chemistry 2023

Published on 16 December 2022. Downloaded on 8/16/2024 8:58:14 AM.

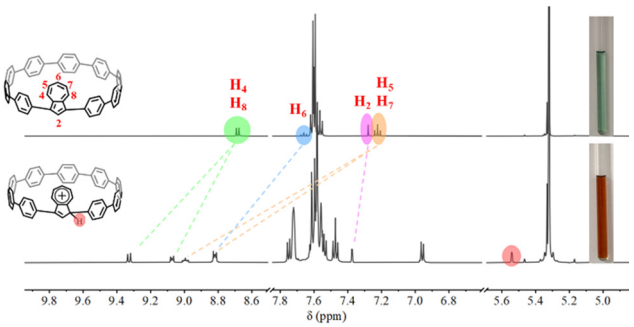

Fig. 3 ^{1}H-NMR spectra and color change of the nanohoop **1,3-Az[9]CPP** before (top) and after protonation (bottom) with 1.0 eq. HBArF·$(Et_2O)_2$ in CD_2Cl_2 (600 MHz, 298 K).

strong deshielding effects due to the formation of an azulenylium cation. Moreover, the proton signals of H4/H8 appear as a doublet peak at 8.70 ppm due to the symmetric structure of the nanohoop, but split into two separate sets of peaks, a doublet peak at 9.34 ppm and a multiplet peak at 9.08 ppm in the protonated asymmetric nanohoop **1,3-Az[9]CPP-H$^+$** (Fig. 3 and S8, ESI†). Similar splits in the triplet peak assigned to H5 and H7 in **1,3-Az[9]CPP** were also observed. Furthermore, a new peak at 5.54 ppm can be assigned to the C–H proton of the protonated five-membered ring. Interestingly, the color of the solution also changed significantly from initially green to yellow and finally deep red with the titrations of HBArF·$(Et_2O)_2$ (Fig. 3 and Fig. S11, ESI†). All these observations demonstrate that the monoprotonation of **1,3-Az[9]CPP** occurs at its C-1 or C-3 position, thus inducing an asymmetric structure of the protonated carbon nanohoop, consistent with the previously reported monoprotonation of azulene derivatives.[26]

Next, we set about investigating the reversible pH stimuli-responsiveness of **1,3-Az[9]CPP**. 1,8-Diazabicyclo[5.4.0]undec-7-ene (DBU) was selected as a base. As shown in Fig. S12 (ESI†), addition of 1.0 equiv. of HBArF·$(Et_2O)_2$ to the **1,3-Az[9]CPP** solution resulted in the disappearance of the proton signals in the azulene unit accompanied by the appearance of the proton signals of azulenylium cations, while the color of the solution turned from green to red. When 1.0 equiv. of DBU was added, the chemical shifts of **1,3-Az[9]CPP** recovered, concomitantly accompanied with the color recovery from red to green (Fig. S12, ESI†). Notably, the process of protonation and deprotonation can be repeated multiple times, indicating the intriguing reversibility of pH stimuli-responsiveness for **1,3-Az[9]CPP**.

The optical properties of **1,3-Az[9]CPP** in the absence and presence of HBArF·$(Et_2O)_2$ were subsequently investigated by UV-vis absorption spectroscopy in a dichloromethane (DCM) solution (Fig. 4a). Furthermore, to gain insight into the relationship between the electronic structure and photophysical properties, time-dependent density functional theory (TD-DFT) calculations were performed at the ωB97XD/6-31g(d,p) level (Fig. S20–S22 and Table S3–S6, ESI†). **1,3-Az[9]CPP** exhibited an absorption maximum (λ_{max}) at 334 nm, which was attributed to the combined transitions of $S_0 \rightarrow S_4$ and $S_0 \rightarrow S_5$ according

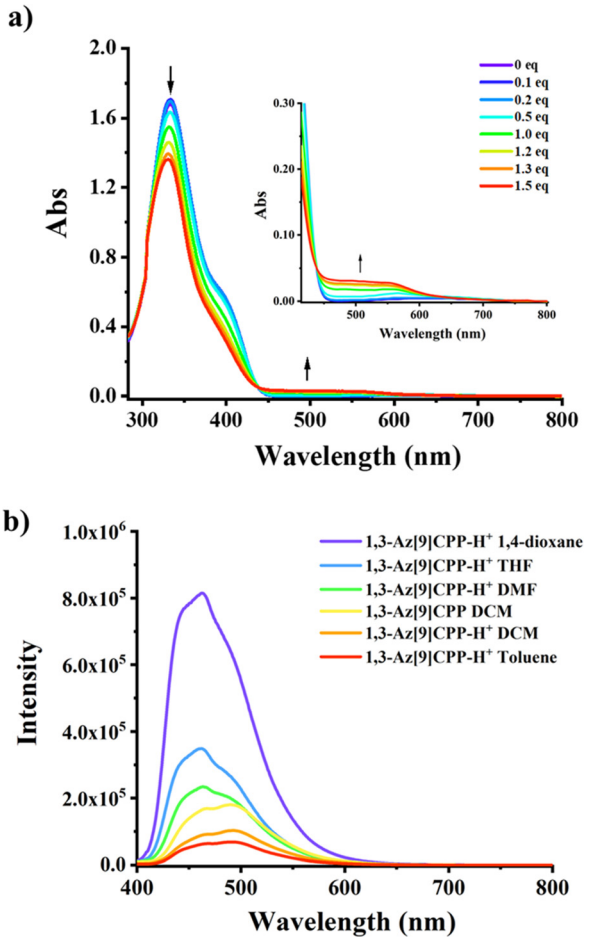

Fig. 4 (a) UV-vis spectra of **1,3-Az[9]CPP** (2.0×10^{-5} M) upon addition of HBArF·$(Et_2O)_2$ in DCM and (b) fluorescence spectra of **1,3-Az[9]CPP** in the absence and presence of 30% TFA (1.0×10^{-5} M) in 1,4-dioxane, THF, DMF, DCM and toluene.

to the TD-DFT calculations. Meanwhile, a shoulder peak appeared at about 385 nm is assigned to the $S_0 \rightarrow S_2$ transition. Moreover, there is a weak broad band at 500–670 nm assigned to the $S_0 \rightarrow S_1$ (HOMO → LUMO) transition, which is consistent with that of the parent azulene.[27] In contrast, significant changes in the UV-vis spectra of **1,3-Az[9]CPP** were observed upon titrations with HBArF·$(Et_2O)_2$ (Fig. 4a). Upon the titrations with acid, the intensity of the peak at λ_{max} decreased remarkably accompanied by a blue-shift of 5 nm from 334 nm to 329 nm. Meanwhile, the intensity of the shoulder peak at 385 nm diminished while a new band at about 497 nm appeared, which is attributed to the generation of azulenium cations. Furthermore, an isosbestic point was clearly observed at 439 nm, implying the existence of two interconverted optically different species in the system. Based on the onset of the longest wavelength absorption (λ_{onset}), the optical gaps of **1,3-Az[9]CPP** and its protonated species were estimated to be 2.74 eV, and 1.82 eV, respectively (Table 1). This tunable optical gap upon protonation/deprotonation was supported by theoretical calculations. In addition, the fluorescence spectrum reveals that **1,3-Az[9]CPP** shows an emission band at around

Published on 16 December 2022. Downloaded on 8/16/2024 8:58:14 AM.

Table 1 Photophysical and electrochemical data of **1,3-Az[9]CPP** and **1,3-Az[9]CPP-H$^+$**

	λ_{abs}[a,b] (nm)	λ_{em}[a,c] (nm)	Φ_F[d] (%)	$E_{g(opt)}$[e] (eV)	E_{HOMO}[f] (eV)
1,3-Az[9]CPP	334	493	1.4	2.74	−4.97
1,3-Az[9]CPP-H$^+$	329	493	1.0	1.82	−4.74

[a] UV-vis absorption and fluorescence spectra were measured in CH_2Cl_2 (1×10^{-5} M) at room temperature. [b] Wavelength of the maximum absorption. [c] Emission maximum (λ_{ex} = highest intensity of absorption plus 10 nm). [d] Absolute fluorescence quantum yield. [e] Estimated from absorption onset, $E_{g(opt)} = 1240/\lambda_{onset}$. [f] $E_{HOMO} = -(4.74 + E_{onset}^{ox})$ eV (calibration by ferrocene).

493 nm. Surprisingly, the emission peak of its protonated species remains almost constant (Fig. 4b). No obvious redshift in emission wavelength can be accounted for by that the cyclic conjugation system of **1,3-Az[9]CPP** in the presence of acid. The excited-state calculation results suggest that the $S_1 \rightarrow S_0$ ($f = 0.0043$) transition of **1,3-Az[9]CPP** is forbidden; hence the emission band at around 445 nm should come from $S_2 \rightarrow S_0$ ($f = 1.18960$) transition of **1,3-Az[9]CPP**, implying the anti-Kasha emission feature. However, in the presence of HBArF·$(Et_2O)_2$, the $S_1 \rightarrow S_0$ ($f = 0.3737$) transition of the protonated **1,3-Az[9]CPP** becomes allowed (Fig. S22 and Table S6, ESI†).

Furthermore, we have also measured UV-vis and fluorescence spectra of **1,3-Az[9]CPP** in the absence and presence of trifluoroacetic acid (TFA) in different solvents including DCM, toluene, N,N-dimethylformamide (DMF), 1,4-dioxane and tetrahydrofuran (THF) (Fig. 4b and Fig. S14, S15, ESI†). Upon titration with TFA, the variations in UV-vis spectra of **1,3-Az[9]CPP** in different solvents were similar to those in DCM but to a different extent (Fig. 4a and Fig. S14, ESI†). Interestingly, a significant increase in fluorescence emission intensity was observed in DMF, 1,4-dioxane and THF solutions (Fig. 4b and Fig. S15, ESI†). The emission intensity in 1,4-dioxane was enhanced to be about 10 times higher than that in DCM at the same emission wavelength (λ_{em}). However, the fluorescence spectrum in toluene is almost the same as that in DCM. These phenomena suggest that polar solvents are more favorable for the fluorescence emission of the azulenylium cation.

The electrochemical properties of **1,3-Az[9]CPP** were further evaluated by CV. In $C_2H_4Cl_2$-Bu_4NPF_6, **1,3-Az[9]CPP** exhibited two oxidation processes. A quasi-reversible peak at 0.28V (peak anode current/peak cathode current, $ip_a/ip_c = 0.3$) and an irreversible peak at 0.79V were observed (Fig. 5). However, in the presence of HBArF·$(Et_2O)_2$, a new reduction peak at −0.58 V was detected, which further confirms the protonation of **1,3-Az[9]CPP**. The CV data in combination with the results of NMR and UV-vis studies confirm that **1,3-Az[9]CPP** features pH reversible stimuli-responsiveness. To the best of our knowledge, it is the first pH-responsive nonalternant all-carbon nanohoop.

The host–guest interaction behaviours between **1,3-Az[9]CPP** and fullerenes C_{60}/C_{70} were finally investigated because **1,3-Az[9]CPP** has a cavity similar to that of [10]CPP.[12] Single crystals of the **C_{60}@1,3-Az[9]CPP** complex suitable for X-ray analysis were prepared by slow diffusion of acetonitrile into a mixed

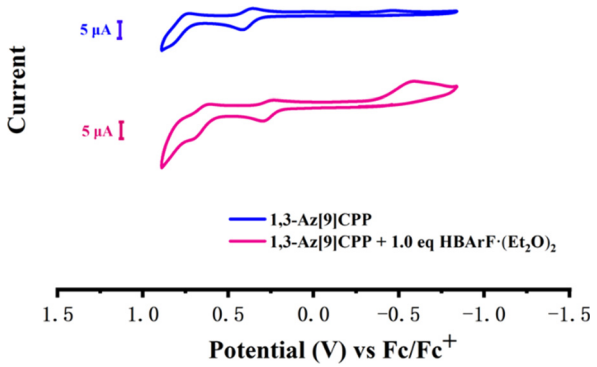

Fig. 5 Cyclic voltammograms of **1,3-Az[9]CPP** (1 mM) and **1,3-Az[9]CPP** upon addition of 1.0 eq. of HBArF·$(Et_2O)_2$ in $C_2H_2Cl_4$ with 0.2 M Bu_4NPF_6 as the supporting electrolyte. The electrode potential was externally calibrated using an Fc/Fc^+ couple.

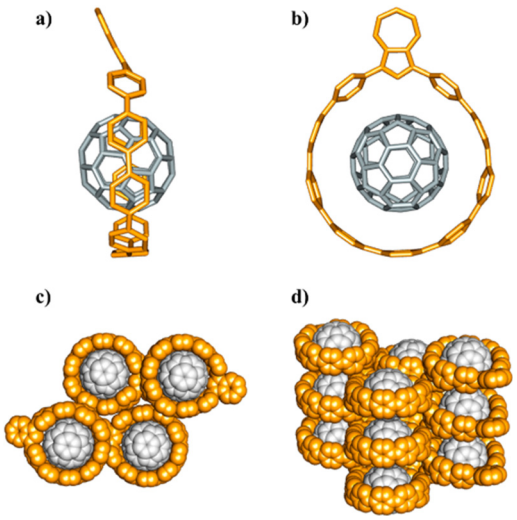

Fig. 6 X-ray crystal structures of **C_{60}@1,3-Az[9]CPP**, (a) side view, (b) top view of the distance between **1,3-Az[9]CPP** and C_{60}, (c) top view and (d) side view of crystal packing showing columnar stacks of C_{60}.

solution of chlorobenzene and CS_2 (Fig. 6). The unit cell of **C_{60}@1,3-Az[9]CPP** belongs to the space group *C*2/*c*. The crystal structure demonstrates that fullerene C_{60} resides inside the cavity of **1,3-Az[9]CPP**, clearly showing a 1 : 1 binding model. The crystal packing shows columnar stacks along the vertical axis (Fig. 6d).

The binding behaviours of **1,3-Az[9]CPP** with C_{60} and C_{70} were further characterized by UV-vis titration experiments in toluene at room temperature. By fitting the UV-vis adsorption changes at 334 nm at different fullerene concentrations, the association constants (K_a) of C_{60} and C_{70} with **1,3-Az[9]CPP** were estimated to be 2.4×10^4 M^{-1} for C_{60} and 1.6×10^4 M^{-1} for C_{70} in toluene (Fig. 7a and Fig. S16a and S17, ESI†), which are smaller than those of 10[CPP] (2.7×10^6 M^{-1} for C_{60} and 8.4×10^4 M^{-1} for C_{70}).[28] The phenomenon is attributed to the tilting of azulene units in the carbon nanohoop. Subsequently, the K_a values of **1,3-Az[9]CPP** with C_{60} and C_{70} in the presence of HBArF·$(Et_2O)_2$ were also extracted by UV-vis titration experiments

 This journal is © The Royal Society of Chemistry 2023

Published on 16 December 2022. Downloaded on 8/16/2024 8:58:14 AM.

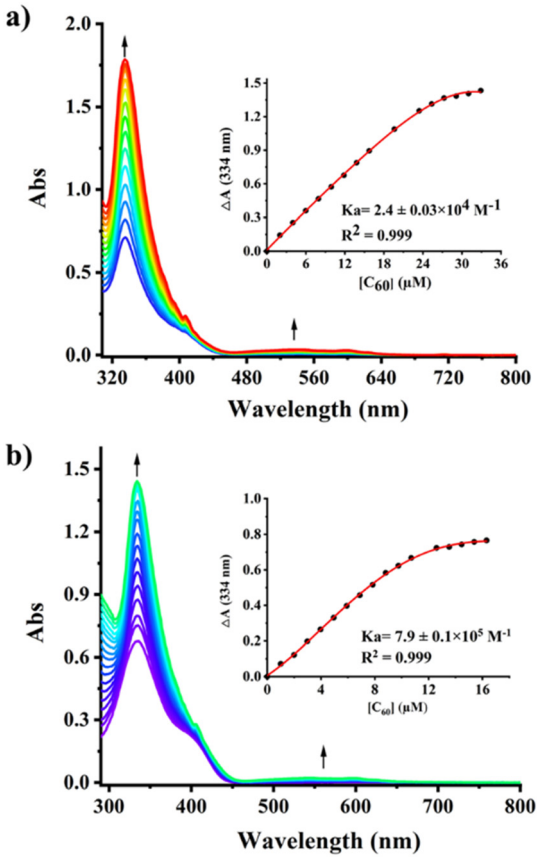

Fig. 7 UV-vis spectra in toluene of (a) **1,3-Az[9]CPP** (1.0×10^{-5} M) in the presence of C_{60} (0–3.29×10^{-5} M), K_a = 2.4×10^4 M^{-1} and (b) **1,3-Az[9]CPP-H$^+$** (1.0×10^{-5} M) in the presence of C_{60} (0–1.63×10^{-5} M), K_a = 7.9×10^5 M^{-1}.

to be 7.9×10^5 M^{-1} and 2.5×10^4 M^{-1} for C_{60} and C_{70}, respectively (Fig. 7b and S16b and S17, ESI†). Notably, K_a of **1,3-Az[9]CPP** with C_{60} in the presence of acid is about 30 times higher than that in the absence of acid, suggesting that the binding of **1,3-Az[9]CPP** to C_{60} was significantly enhanced in the presence of acid. This enhanced binding can be accounted for the cation–π interaction between the aromatic tropylium ion and the fullerene rich in π-electrons. This interpretation was verified by NMR titration (Fig. S18 and S19, ESI†). As for **C_{60}@1,3-Az[9]CPP-H$^+$** and **C_{70}@1,3-Az[9]CPP-H$^+$**, due to the enhanced electronic shielding by cation–π-electron interaction, the proton signals of H4'/H8' and H6' attributed to the protonated azulene are observed to have moved to higher fields. Moreover, the perfect size match between **1,3-Az[9]CPP-H$^+$** and symmetrical spherical structure C_{60} may also make an important contribution for a favorable binding interaction. This acid-tunable selectivity of **1,3-Az[9]CPP** for C_{60} over C_{70} may have potential application in enriching C_{60} from fullerene C_{60}/C_{70} mixtures.[29]

Conclusions

In summary, we have successfully synthesized the first conjugated nonalternant all-carbon nanohoop by incorporating an azulene unit. The data demonstrated that the 1,3-azulene-embedded carbon nanohoop exhibits quite unique optical and physical properties such as anti-Kasha's rule emission and an adjustable band gap. Notably, **1,3-Az[9]CPP** also shows good pH reversible stimuli-responsiveness and this process of protonation and deprotonation can be repeated multiple times. Remarkably, in an acidic environment, **1,3-Az[9]CPP** shows a high selectivity (30/1) in binding of C_{60} over C_{70}. This work can motivate further investigations of conjugated nanohoops containing nonalternant π-systems and develop their potential application in the field of host–guest chemistry as well as functional materials. Currently, incorporations of 2,6- and 4,7- connected azulene units into the CPP skeleton are ongoing projects in our laboratory.

Author contributions

X. L. performed the experiments, carried out the characterization, and collected and analyzed the data. L. J. and Y. W. performed the theoretical calculations. W. W. analyzed the data of the electrochemical section. D. S. processed the single crystal data. H. J. and X. L. wrote the manuscript. All authors participated in the discussion and revised the manuscript.

Conflicts of interest

The authors declare no competing financial interests.

Acknowledgements

We are grateful for the financial support from the National Natural Science Foundation of China (21971020) and the Beijing Natural Science Foundation (2212008).

Notes and references

1 (*a*) R. Jasti and C. R. Bertozzi, *Chem. Phys. Lett.*, 2010, **494**, 1–7; (*b*) U. H. Bunz, S. Menning and N. Martin, *Angew. Chem., Int. Ed.*, 2012, **51**, 7094–7101; (*c*) H. Omachi, T. Nakayama, E. Takahashi, Y. Segawa and K. Itami, *Nat. Chem.*, 2013, **5**, 572–576; (*d*) H. Chen and Q. Miao, *J. Phys. Org. Chem.*, 2020, **33**, e4145.

2 R. Jasti, J. Bhattacharjee, J. B. Neaton and C. R. Bertozzi, *J. Am. Chem. Soc.*, 2008, **130**, 17646–17647.

3 (*a*) S. E. Lewis, *Chem. Soc. Rev.*, 2015, **44**, 2221–2304; (*b*) E. R. Darzi and R. Jasti, *Chem. Soc. Rev.*, 2015, **44**, 6401–6410; (*c*) Y. Segawa, A. Yagi, K. Matsui and K. Itami, *Angew. Chem., Int. Ed.*, 2016, **55**, 5136–5158; (*d*) E. J. Leonhardt and R. Jasti, *Nat. Rev. Chem.*, 2019, **3**, 672–686; (*e*) I. Roy, A. H. G. David, P. J. Das, D. J. Pe and J. F. Stoddart, *Chem. Soc. Rev.*, 2022, **51**, 5557–5605.

4 (*a*) H. Omachi, Y. Segawa and K. Itami, *Org. Lett.*, 2011, **13**, 2480–2483; (*b*) Z. Sun, T. Suenaga, P. Sarkar, S. Sato, M. Kotani and H. Isobe, *Proc. Natl. Acad. Sci. U. S. A.*, 2016, **113**, 8109–8114; (*c*) K. Okada, A. Yagi, Y. Segawa and

Published on 16 December 2022. Downloaded on 8/16/2024 8:58:14 AM.

K. Itami, *Chem. Sci.*, 2017, **8**, 661–667; (*d*) H. Jia, Y. Gao, Q. Huang, S. Cui and P. Du, *Chem. Commun.*, 2018, **54**, 988–991.

5 (*a*) P. Li, B. M. Wong, L. N. Zakharov and R. Jasti, *Org. Lett.*, 2016, **18**, 1574–1577; (*b*) P. Della Sala, A. Capobianco, T. Caruso, C. Talotta, M. De Rosa, P. Neri, A. Peluso and C. Gaeta, *J. Org. Chem.*, 2018, **83**, 220–227.

6 T. Iwamoto, E. Kayahara, N. Yasuda, T. Suzuki and S. Yamago, *Angew. Chem., Int. Ed.*, 2014, **53**, 6430–6434.

7 (*a*) E. Kayahara, R. Qu, M. Kojima, T. Iwamoto, T. Suzuki and S. Yamago, *Chem. – Eur. J.*, 2015, **21**, 18939–18943; (*b*) L. Sicard, O. Jeannin, J. Rault-Berthelot, C. Quinton and C. Poriel, *ChemPlusChem*, 2018, **83**, 874–880; (*c*) L. Sicard, F. Lucas, O. Jeannin, P. A. Bouit, J. Rault-Berthelot, C. Quinton and C. Poriel, *Angew. Chem., Int. Ed.*, 2020, **59**, 11066–11072.

8 Y. Y. Liu, J. Y. Lin, Y. F. Bo, L. H. Xie, M. D. Yi, X. W. Zhang, H. M. Zhang, T. P. Loh and W. Huang, *Org. Lett.*, 2016, **18**, 172–175.

9 (*a*) J. M. Van Raden, B. M. White, L. N. Zakharov and R. Jasti, *Angew. Chem., Int. Ed.*, 2019, **58**, 7341–7345; (*b*) J. M. Van Raden, N. N. Jarenwattananon, L. N. Zakharov and R. Jasti, *Chem. – Eur. J.*, 2020, **26**, 10205–10209.

10 T. Kuwabara, J. Orii, Y. Segawa and K. Itami, *Angew. Chem., Int. Ed.*, 2015, **54**, 9646–9649.

11 (*a*) D. Lu, H. Wu, Y. Dai, H. Shi, X. Shao, S. Yang, J. Yang and P. Du, *Chem. Commun.*, 2016, **52**, 7164–7167; (*b*) Q. Huang, G. Zhuang, H. Jia, M. Qian, S. Cui, S. Yang and P. Du, *Angew. Chem., Int. Ed.*, 2019, **58**, 6244–6249.

12 Y. Xu and M. von Delius, *Angew. Chem., Int. Ed.*, 2020, **59**, 559–573.

13 J. He, M. Yu, M. Pang, Y. Fan, Z. Lian, Y. Wang, W. Wang, Y. Liu and H. Jiang, *Chem. – Eur. J.*, 2022, **28**, e202103832.

14 S. Hitosugi, S. Sato, T. Matsuno, T. Koretsune, R. Arita and H. Isobe, *Angew. Chem., Int. Ed.*, 2017, **56**, 9106–9110.

15 P. Du, Q. Huang, Y. Wu, Y. Zhou, H. Liu, J. Wang and S. Wang, *Synthesis*, 2020, 2535–2540.

16 (*a*) D. Wassy, M. Pfeifer and B. Esser, *J. Org. Chem.*, 2020, **85**, 34–43; (*b*) J. S. Wossner, D. Wassy, A. Weber, M. Bovenkerk, M. Hermann, M. Schmidt and B. Esser, *J. Am. Chem. Soc.*, 2021, **143**, 12244–12252.

17 Y. Li, Y. Segawa, A. Yagi and K. Itami, *J. Am. Chem. Soc.*, 2020, **142**, 12850–12856.

18 (*a*) A. Pfau and P. A. Plattner, *Helv. Chim. Acta*, 1939, **22**, 202–208; (*b*) M. Beer and H. C. Longuet-Higgins, *J. Chem. Phys.*, 1955, **23**, 1390–1391; (*c*) J. Michl and E. W. Thulstrup, *Tetrahedron*, 1976, **32**, 205–209; (*d*) R. S. H. Liu, *J. Chem. Educ.*, 2002, **79**, 183–185; (*e*) J. C. Del Valle and J. Catalan, *Phys. Chem. Chem. Phys.*, 2019, **21**, 10061–10069; (*f*) H. Wang, J. Wang, T. Zhang, Z. Xie, X. Zhang, H. Sun, Y. Xiao, T. Yu and W. Huang, *J. Mater. Chem. C*, 2021, **9**, 10154–10172; (*g*) K. Veys and D. Escudero, *Acc. Chem. Res.*, 2022, **55**, 2698–2707.

19 S. S. Danyluk and W. G. Schneider, *Can. J. Chem.*, 1962, **40**, 1777–1785.

20 (*a*) Y. Yamaguchi, K. Ogawa, K. Nakayama, Y. Ohba and H. Katagiri, *J. Am. Chem. Soc.*, 2013, **135**, 19095–19098; (*b*) Y. Yamaguchi, M. Takubo, K. Ogawa, K. Nakayama, T. Koganezawa and H. Katagiri, *J. Am. Chem. Soc.*, 2016, **138**, 11335–11343; (*c*) H. Ran, X. Duan, R. Zheng, F. Xie, L. Chen, Z. Zhao, R. Han, Z. Lei and J.-Y. Hu, *ACS Appl. Mater. Interfaces*, 2020, **12**, 23225–23235; (*d*) H. Xin, B. Hou and X. Gao, *Acc. Chem. Res.*, 2021, **54**, 1737–1753; (*e*) H. Ran, F. Li, R. Zheng, H. Zhang, F. Xie, P. Jin, Z. Lei, X.-T. Wang and J.-Y. Hu, *Dyes Pigm.*, 2022, **203**, 110311.

21 A. G. Lvov and A. Bredihhin, *Org. Biomol. Chem.*, 2021, **19**, 4460–4468.

22 (*a*) Y.-Y. He, J. Chen, X.-L. Zheng, X. Xu, W.-Q. Li, L. Yang and W. Q. Tian, *ACS Appl. Nano Mater.*, 2019, **2**, 1648–1654; (*b*) C.-C. Yang, J.-Y. Ma, X. Su, X.-L. Zheng, J. Chen, Y.-Y. He, W. Quan Tian, W.-Q. Li and L. Yang, *FlatChem*, 2022, **33**, 100362.

23 (*a*) C. M. Lopez-Alled, A. Sanchez-Fernandez, K. J. Edler, A. C. Sedgwick, S. D. Bull, C. L. McMullin, G. Kociok-Kohn, T. D. James, J. Wenk and S. E. Lewis, *Chem. Commun.*, 2017, **53**, 12580–12583; (*b*) L. C. Murfin and S. E. Lewis, *Molecules*, 2021, **26**, 353.

24 (*a*) N. Ogawa, Y. Yamaoka, H. Takikawa, K. I. Yamada and K. Takasu, *J. Am. Chem. Soc.*, 2020, **142**, 13322–13327; (*b*) S. Mishra, T. G. Lohr, C. A. Pignedoli, J. Liu, R. Berger, J. I. Urgel, K. Mullen, X. Feng, P. Ruffieux and R. Fasel, *ACS Nano*, 2018, **12**, 11917–11927; (*c*) I. C. Hou, Q. Sun, K. Eimre, M. Di Giovannantonio, J. I. Urgel, P. Ruffieux, A. Narita, R. Fasel and K. Mullen, *J. Am. Chem. Soc.*, 2020, **142**, 10291–10296; (*d*) C. Duan, J. Zhang, J. Xiang, X. Yang and X. Gao, *Angew. Chem., Int. Ed.*, 2022, **61**, e202201494; (*e*) S. Wang, M. Tang, L. Wu, L. Bian, L. Jiang, J. Liu, Z. B. Tang, Y. Liang and Z. Liu, *Angew. Chem., Int. Ed.*, 2022, e202205658.

25 Y. Segawa, H. Omachi and K. Itami, *Org. Lett.*, 2010, **12**, 2262–2265.

26 (*a*) J. Schulze and F. A. Long, *J. Am. Chem. Soc.*, 1963, **86**, 322–326; (*b*) F. Wang, T. T. Lin, C. He, H. Chi, T. Tang and Y.-H. Lai, *J. Mater. Chem.*, 2012, **22**, 10448.

27 M. Koch, O. Blacque and K. Venkatesan, *J. Mater. Chem. C*, 2013, **1**, 7400.

28 (*a*) T. Iwamoto, Y. Watanabe, T. Sadahiro, T. Haino and S. Yamago, *Angew. Chem., Int. Ed.*, 2011, **50**, 8342–8344; (*b*) T. Iwamoto, Y. Watanabe, H. Takaya, T. Haino, N. Yasuda and S. Yamago, *Chem. – Eur. J.*, 2013, **19**, 14061–14068.

29 W. Sun, Y. Wang, L. Ma, L. Zheng, W. Fang, X. Chen and H. Jiang, *J. Org. Chem.*, 2018, **83**, 14667–14675.

 This journal is © The Royal Society of Chemistry 2023